Int J Clin Exp Med 2019;12(1):304-315
www.ijcem.com /ISSN:1940-5901/IJCEM0074378

Original Article

Ginsenoside Rg1 protects steroid-induced osteonecrosis of the femoral head in rats by suppressing oxidative stress and adipogenesis

Ke Heng[1], Yunxia Zhu[2], Qinghe Geng[3], Guoyong Yin[4], Xiao Han[2]

[1]Department of Orthopedics, The Affiliated Changzhou No. 2 People's Hospital of Nanjing Medical University, Changzhou, P. R. China; [2]Key Laboratory of Human Functional Genomics of Jiangsu Province, Nanjing Medical University, Nanjing, China; [3]Department of Orthopedics, The People's Hospital of Pizhou, Xuzhou Medical University, Xuzhou, P. R. China; [4]Department of Orthopedics, The First Affiliated Hospital of Nanjing Medical University, Nanjing, P. R. China

Received February 10, 2018; Accepted October 11, 2018; Epub January 15, 2019; Published January 30, 2019

Abstract: This study aimed to investigate the effects of ginsenoside Rg1 (Rg1) in preventing steroid-induced osteonecrosis. Forty-five adult rats were randomly divided into a control group, a model group, and an Rg1 group. Each group included 15 rats. In the model and Rg1 groups, a high dose of methylprednisolone acetate (40 mg/kg) was injected once into the gluteus medius muscle. In the Rg1 group, Rg1 was administered every day for 6 weeks after the methylprednisolone acetate injection. The pathological, microstructural, biochemical and phenotype parameters were analyzed. The ratio of empty lacuna and adipose tissue in the bone marrow were significantly lower in the Rg1 group than in the model group. The microfocal-computed tomography results indicated that Rg1 improved the microstructure of the trabecular bone and increased bone mineral density in rats with steroid-induced osteonecrosis of the femoral head (ONFH). Rg1 also significantly improved hyperlipidemia in the steroid-induced ONFH rats. Moreover, Rg1 enhanced femoral head neovascularization by preventing blood vessel loss. Rg1 suppressed oxidative stress and adipogenesis in the femoral heads of the steroid-induced ONFH rats. Rg1 may protect rats against steroid-induced ONFH by suppressing oxidative stress and adipogenesis.

Keywords: Ginsenoside Rg1, steroid-induced osteonecrosis, oxidative stress, adipogenesis

Introduction

Steroid-induced osteonecrosis of the femoral head (ONFH) is a chronic destructive disease of the hip joints. Steroid-induced osteonecrosis develops in patients who receive long-term or high-dose glucocorticoids for acute lymphoblastic leukemia, renal transplantation, rheumatoid arthritis, and systemic lupus erythematosus [1, 2].

Based on the stage of steroid-induced osteonecrosis of the femoral head, a variety of treatments can be used, such as reducing weight bearing, drug therapies, core decompression with or without bone marrow cell transplantation, and total hip replacement [3]. However, all of these techniques only focus on preventing irreversible complications. New, more efficient methods with fewer complications are urgently required. Over the past several years, drug therapies, such as statins [4] and antioxidative substances including Vitamin E [5] have been used to treat ONFH *in vivo* and *in vitro* animal models by suppressing adipogenesis and oxidative injury. Therefore, the ability of inhibiting adipogenesis and oxidative stress may be a crucial part of treatment in ONFH.

Rg1 is one of the active ingredients in ginsenosides, which are the principal pharmacologically-active components of Panax ginseng, a well-known traditional Chinese herbal medicine [6]. Rg1 has garnered attention due to its powerful ability to regulate diverse physiological processes. The pharmacological potentials of Rg1 include, but are not limited to, reducing oxidative stress [7], suppressing adipogenesis [8]

and promoting anti-inflammatory activity [9] anti-apoptosis activity [10], pro-proliferation [11], and neuroprotection [12] via signaling pathways, such as Akt-FoxO3a-Bim, estrogen receptors, Wnt-β-catenin, and peroxisome proliferator-activated receptor (PPARγ)-HO-1 [11, 13-15].

Although there is currently no clear evidence on the effects of Rg1 in steroid-induced ONFH, researchers have reported that Rg1 can attenuate fat accumulation and promote angiogenesis and osteogenesis [16-18], which are key processes involved in the treatment of steroid-induced ONFH. However, as a well-known nuclear receptor, peroxisome proliferator-activated receptor (PPARγ) can promote adipogenesis and lipid metabolism in adipose tissue and inhibit oxidative stress in the regulation of vascular tone in endothelial cells [19-21], providing a molecular basis against steroid-induced ONFH.

Therefore, the present study aimed to identify whether Rg1 can prevent steroid-induced ONFH by suppressing oxidative injury and adipogenesis.

Materials and methods

Study animals

Forty-five 8-week-old male Sprague-Dawley (SD) rats, weighing 370-410 g, were obtained from the Experimental Animal Center of Nanjing Medical University in Nanjing, China. All the rats were kept in a clean room with an air filtration system. The animals' cages and water were disinfected. All experimental procedures were performed in accordance with guidelines established by the Research Animal Care Committee of Nanjing Medical University, in Nanjing, China.

Study groups and treatment

After a one-week period of feeding adaptation, the rats were accurately weighed and randomly assigned to three groups: a control group (n = 15), a model group (steroid-induced ONFH rats, n = 15), and an Rg1 group (steroid-induced ONFH rats, treated with 20 mg/kg Rg1, n = 15). One high dose of methylprednisolone acetate (MPSL) (40 mg/kg; Pfizer Manufacturing Belgium NV, Puurs, Belgium) was administered once to the gluteus medius muscle of the rats to induce osteonecrosis. After the MPSL injection, the rats in the Rg1 group received an intraperitoneal injection of 1.5 mL Rg1 (Shanghai Oriental Pharmaceutical Co. Ltd., Shanghai, China) every day for six weeks. In the control and model groups, the rats were fed a normal diet. All the experiments were approved by and performed in compliance with the Research Animal Care and Use Committee of Nanjing Medical University.

Tissue sample preparation

The rats in each group were sacrificed six weeks after the MPSL injection. The rats were anaesthetized using an intravenous injection of trichloroacetaldehyde hydrate (0.3 mL/kg, Sinopharm Chemical Reagent Suzhou Co. Ltd, China); they were then euthanized by exsanguination via aortectomy. To conduct the light microscopic examinations and the microfocal-computed tomography (Micro-CT) scans, bilateral femoral bones were obtained at the time of death, and the left side of the bone samples was fixed for three days in 4% paraformaldehyde (pH 7.4). After scanning, the bone samples were decalcified with 10% EDTA for 28 days. The samples were sectioned along the proximal one-third of the coronal plane and cut along the distal part (condyle) of the axial plane. Finally, the specimens were embedded in paraffin, cut into 5 mm sections, and stained with hematoxylin and eosin. The right side of the bone samples were stored at -80°C for real-time polymerase chain reaction (PCR) and Western blot analyses.

Evaluation of steroid-induced ONFH

The osteonecrotic changes and repair processes in the steroid-treated rats were evaluated using histopathological examination six weeks after the MPSL injection. The slides were observed by three, blinded independent observers. Osteonecrosis was identified when necrosis of the medullary hematopoietic cells or fat cells was observed or when empty lacunae or condensed nuclei were seen in the osteocytes. The empty lacunae ratio (empty lacunae/the total number of osteocytes) was calculated for each femoral head using a coronal section taken at the maximal femoral width. During the observation of the fat cells in bone marrow, the fat tissue area was also calculated. Image Pro

Plus 6.0 image analysis software was used for the calculation.

Hematological examination

To observe the hyperlipidemia-improving effects of Rg1, blood samples were collected from the abdominal aorta six weeks after the MPSL injection. The serum levels of total triglycerides (TG), total cholesterol (TC), low-density lipoprotein (LDL), high-density lipoprotein (HDL), apolipoprotein A1 (ApoA1), and apolipoprotein B (ApoB) were determined. The levels of lipid peroxidation (LPO), superoxide dismutase (SOD), catalase (CAT), and glucose-6-phosphate dehydrogenase (G6PHD) were also determined to provide evidence for the effect of Rg1 on the blood antioxidant status six weeks after the Rg1 injection.

Micro-CT scanning

Micro-CT (μCT, GE Healthcare Biosciences, Piscataway, NJ, USA) was used to measure the micro-structure of the femoral heads [22]. The following parameters were used to quantified the relative amount of bone: bone volume/total volume (BV/TV), trabecular thickness (Tb.Th), trabecular bone pattern factor (Tb.Pf), trabecular number (Tb.N), trabecular separation (Tb.Sp), and bone mineral density (BMD).

Quantification of microvessel density

Microvessel density (MVD), a measure of angiogenesis, was determined using light microscopy after immunostaining sections with anti-CD31 antibodies according to the procedure described in [23]. The microvessels were counted on a 200× field. Any single endothelial cell or cluster of endothelial cells that were clearly separated from the adjacent microvessels was counted as one microvessel. In all, 10 representative areas of the section were counted. The evaluation was performed by two researchers who were blinded to the identity of the Rg1 group.

Immunohistochemical staining

Paraffin sections from the femoral head samples were incubated for 10 min with 3% H_2O_2. For antigen retrieval, the sections were immersed in 0.1% trypsinase solution at 37°C for 5-30 min. After incubation with 10% goat anti-serum (Vector, Burlingame, CA, USA) for 30 min at 25°C, the sections were treated with a primary antibody against rat CD31, PPARγ or vascular endothelial growth factor (VEGF) (all rabbit antibodies were obtained from Santa Cruz Biotechnology, Inc., Dallas, Texas, USA) for 14 h at 4°C. The samples were then treated with a biotin-labeled secondary antibody for 30 min, and then incubated with horseradish peroxidase-conjugated streptavidin for 30 min at 25°C. After counterstaining with hematoxylin, the sections were dehydrated and mounted. Appropriate sections were selected for use as the positive and negative controls. To locate and identify the areas with positively stained cells, Image-Pro Plus 6.0 was used at a magnification of 9200. Random fields in the bone marrow cavities were chosen for VEGF staining. Positive staining was quantified based on integrated optical density (IOD). The corresponding area was also metered. The results were defined as the ratio of IOD to the corresponding area.

Western blot analysis

The protein expression levels of PPARγ, Prdx1, SOD1, and SOD2 in the femoral head tissues obtained from the rats in all three groups were detected using Western blot analysis. Total protein (20 μg/lane) was first separated using 10% sodium dodecyl sulfate polyacrylamide gel electrophoresis and then transferred onto polyvinylidene fluoride blotting membranes. The primary antibody was incubated on the membrane for 12 h at 4°C after non-specific blocking with 5% bovine serum albumin in Tween-Tris Buffered Saline. The following primary antibodies were used: PPARγ antibody (rabbit antibody, dilution 1:500, Santa Cruz Biotechnology, Inc., Santa Cruz, CA, USA), β-actin antibody (internal control, rabbit polyclonal antibody, dilution 1:5000, Santa Cruz Biotechnology, Inc., Santa Cruz, CA, USA), Prdx1 antibody (rabbit antibody, dilution 1:1000, Millipore Corporation, Billerica, MA, USA), SOD1 antibody (rabbit antibody, dilution 1:500, Cell Signaling Technology, Inc., Danvers, MA, USA), SOD2 antibody (rabbit antibody, dilution 1:1000, Cell Signaling Technology, Inc., Danvers, MA, USA), and glyceraldehyde-3-phosphate dehydrogenase antibody (internal control, rabbit polyclonal antibody, dilution 1:5000, Santa Cruz Biotechnology, Inc., Santa Cruz, CA, USA). The membranes were then

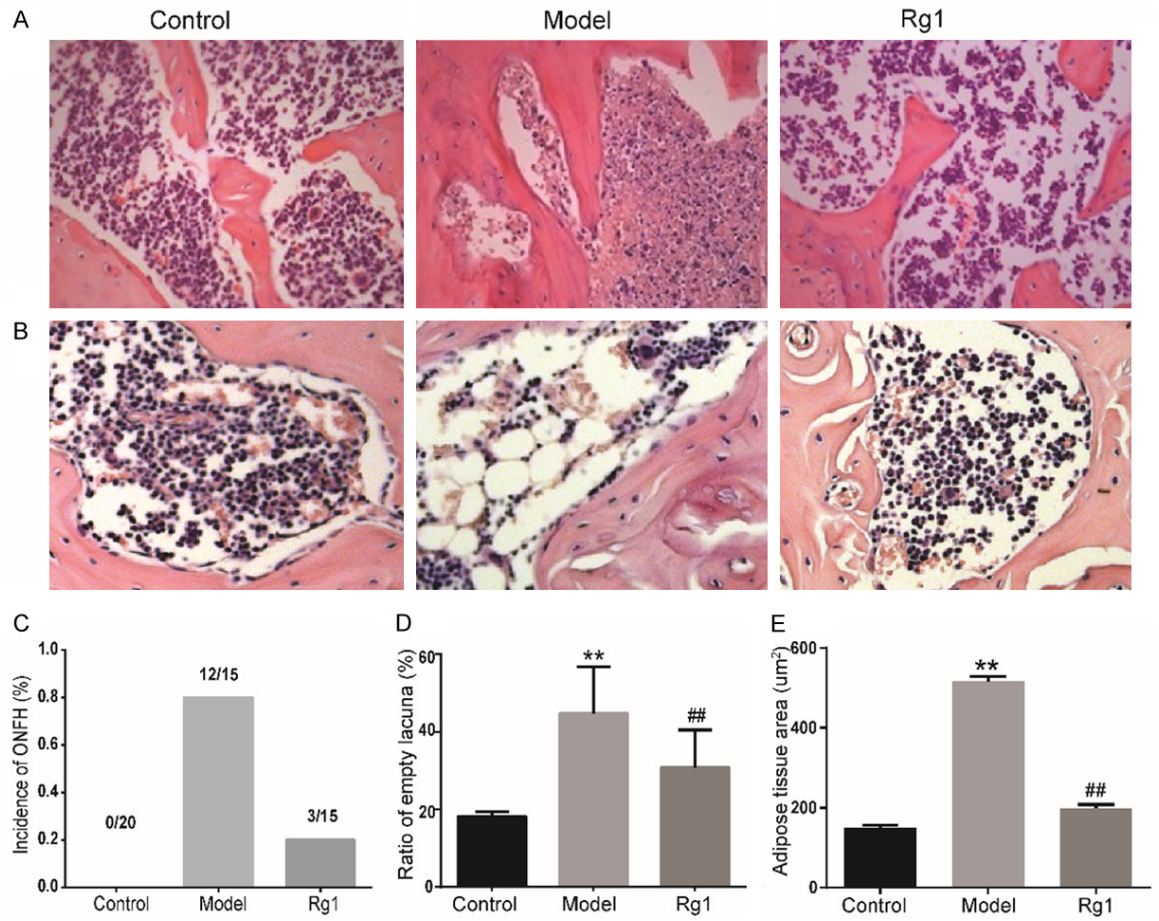

Figure 1. Rg1 reduces the histopathological results in rats with steroid-induced osteonecrosis of the femoral head (ONFH). A: histopathological examination staining of the femoral head from the control group, the model group, and the Rg1 group. B: The adipose tissue area in the bone marrow was significantly higher in the model group than the Rg1 and control groups. C: The incidence of ONFH was significantly lower in the Rg1 group than the model group (Fisher's exact probability test, $P < 0.01$). Statistical analysis of the differences of the ratio of empty lacuna (D) and adipose tissue area (E) in the control, model, and Rg1 groups. Data are presented as the mean ± S.D. (n = 15 for the control group, n = 15 for the model group, n = 15 for the Rg1 group). **: $P < 0.01$, in comparison to the control group. ##: $P < 0.01$, in comparison to the model group. Magnification: ×200 (A, B).

treated with horseradish peroxidase-labeled secondary antibody (ZDR-5306; Zhongshan Golden Bridge Biotechnology, Beijing, China) for 2 h at 37°C. The immuno-reactive proteins on the blots were visualized with ECL™ Western blotting detection reagents (GE Healthcare Life Sciences, Pittsburgh, PA, USA), and the signals were analyzed using Image Station 4000R (Kodak, Rochester, New York, USA).

Statistical analysis

Statistical Package for the Social Sciences (SPSS) version 16.0 for Windows (SPSS Inc., Chicago, IL, USA) were used for the statistical analysis. The data were expressed as the mean ± standard deviation. A one-way analysis of variance (ANOVA) followed by the least significant difference (LSD) test was performed to compare the means among multiple groups. Fisher's exact probability test was used for the incidence of osteonecrosis. A value of $P < 0.05$ was considered statistically significant.

Results

Rg1 reduces histopathological changes in steroid-induced ONFH rats

The histological results indicated that osteonecrosis was observed in 12 of the 15 rats in the model group and in three of the 15 rats in the

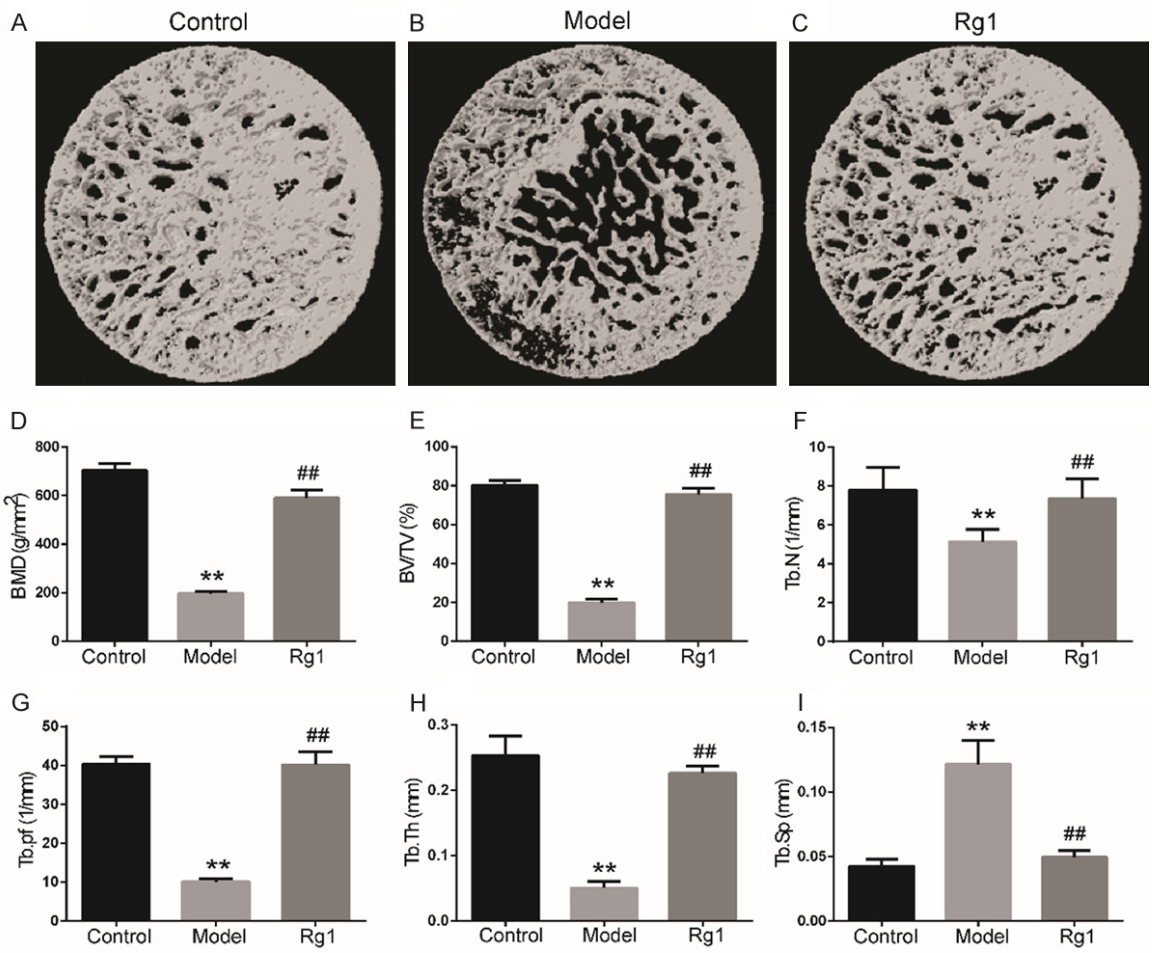

Figure 2. Rg1 prevents bone loss in steroid-induced ONFH in rats. Micro-CT bone scanning results from the control, model, and Rg1 groups (A-C). (E) bone volume/total volume (BV/TV), (H) trabecular thickness (Tb.Th), (G) trabecular bone pattern factor (Tb.Pf), (F) trabecular number (Tb.N), and (D) bone mineral density (BMD) were significantly increased in the Rg1 group in comparison to the model group, while (I) trabecular separation (Tb.Sp) in the Rg1 group was significantly reduced. The data are presented as the mean ± SD (n = 15 for the control group, n = 15 for the model group, n = 15 for the Rg1 group). **: $P < 0.01$, in comparison to the control group. ##: $P < 0.01$, in comparison to the model group.

Rg1 group. The incidence of osteonecrosis was significantly lower in the Rg1 group than the model group (Fisher's exact probability test, $P < 0.01$, **Figure 1C**). No rats in the control group were diagnosed with osteonecrosis. The osteonecrotic changes and repair processes of the rats in each group were histologically examined to evaluate the effects of Rg1 on steroid-induced ONFH. In comparison to the control group, an accumulation of bone marrow cell debris was found in the ONFH lesions in the model group, while Rg1 dramatically attenuated this change in the rats with steroid-induced ONFH (**Figure 1A**). In addition, the empty lacunae ratio was significantly higher in the model group than the Rg1 and control groups. ($P < 0.01$, n = 15, **Figure 1D**). Moreover, as shown in **Figure 1B**, the adipose tissue area in the bone marrow was significantly higher in the model group than the Rg1 and control groups ($P < 0.01$, n = 15, **Figure 1E**).

Rg1 prevents bone loss in steroid-induced ONFH rats

We used micro-CT bone scanning to analyze the bone structure in the femoral heads of the rats (**Figure 2A-C**). The BV/TV ($P < 0.01$, **Figure 2E**), Tb.Th ($P < 0.01$, **Figure 2H**), Tb.Pf ($P < 0.01$, **Figure 2G**), and Tb.N ($P < 0.01$, **Figure 2F**) volumes were significantly increased in the Rg1 group in comparison to the model group, while

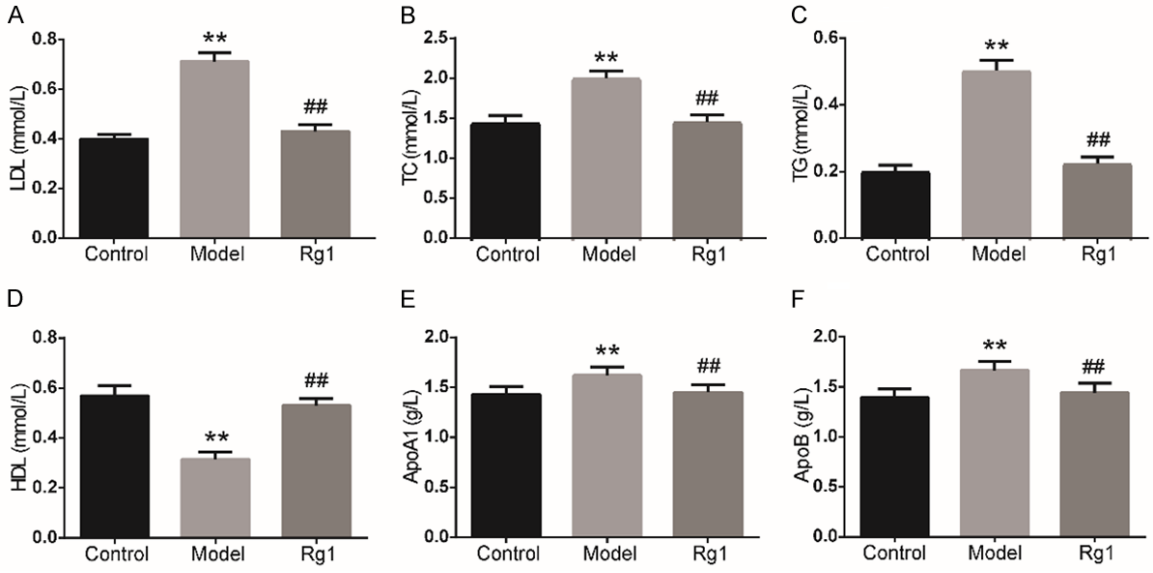

Figure 3. Rg1 improves hyperlipidemia in steroid-induced ONFH rats. Rg1 significantly reduced hyperlipidemia by decreasing LDL (A), TC (B), TG (C), ApoA1 (E), and ApoB (F) levels, and increasing HDL levels (D). The data are presented as the mean ± SD (n = 15 for the control group, n=15 for the model group, n = 15 for the Rg1 group). **: P < 0.01, in comparison to the control group. ##: P < 0.01, in comparison to the model group.

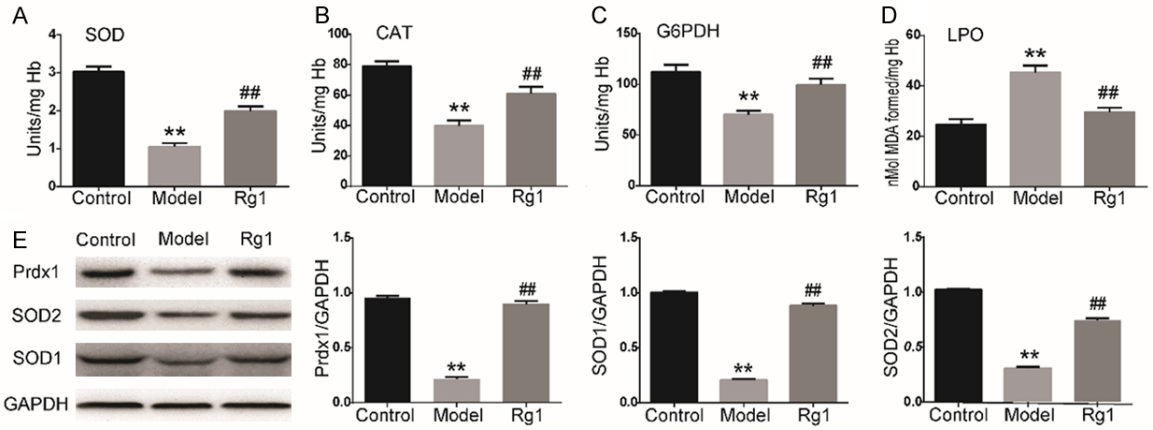

Figure 4. The antioxidant status of the steroid-induced ONFH rats. The SOD, G6PDH, and CAT activities were significantly higher in the Rg1 group than the model group (A-C). LPO levels were significantly higher in the model group than the control and Rg1 groups (D). The Prdx1, SOD1, and SOD2 protein expression levels were significantly reduced in the model group in comparison to the Rg1 and control group in Western blot analysis (E). The data are presented as the mean ± SD (n = 15 for the control group, n = 15 for the model group, n = 15 for the Rg1 group). **: P < 0.01, in comparison to the control group. ##: P < 0.01, in comparison to the model group.

the Tb.Sp (P < 0.01, **Figure 2I**) was significantly reduced. We also measured the BMD values. The rats in the model group showed markedly reduced BMD in the femoral head in comparison to the rats in the control group (P < 0.01, **Figure 2D**). The BMD values in the rats treated with Rg1 were higher than the rats in the model group that did not undergo drug treatment (P < 0.01, **Figure 2D**).

Rg1 improves hyperlipidemia in steroid-induced ONFH rats

The blood chemistry data showed that the rats in the Rg1 and model groups had significantly higher concentrations of serum TG, TC, LDL, ApoA1, and ApoB and significantly lower levels of HDL than the rats in the control group. In comparison to the model group, hyperlipidemia

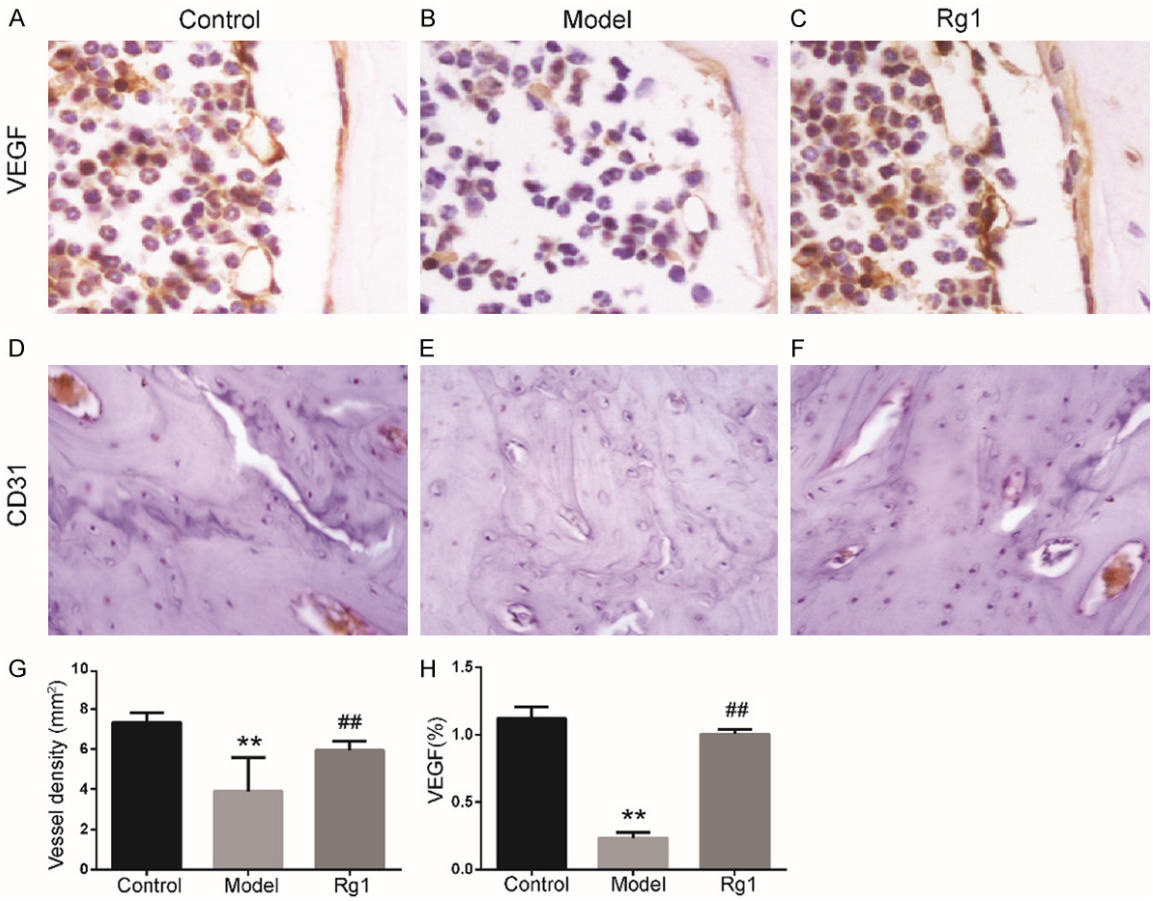

Figure 5. Rg1 promotes angiogenesis in steroid-induced ONFH in rats. Immunohistochemical staining of VEGF and CD31 was less intense in the model group (B, E) than the Rg1 (C, F) and control groups (A, D). Significant statistical differences in microvessel density (MVD) were found between the Rg1 group and the model group (G). Immunohistochemical staining for VEGF was significantly lower in the model group than the control and Rg1 groups (H). The data are presented as the mean ± SD (n = 15 for the control group, n = 15 for the model group, n = 15 for the Rg1 group). **: P < 0.01, in comparison to the control group. ##: P < 0.01, in comparison to the model group. Magnification: ×400 (A-C), ×200 (D-F).

in the Rg1 group improved, as evidenced by decreases in the TG (P < 0.01, **Figure 3C**), TC (P < 0.01, **Figure 3B**), LDL (P < 0.01, **Figure 3A**), ApoA1 (P < 0.01, **Figure 3E**), and ApoB (P < 0.01, **Figure 3F**) levels, and increases in the HDL levels (P < 0.01, **Figure 3D**).

Rg1 inhibits oxidative stress in steroid-induced ONFH rats

The SOD, G6PDH, and CAT activities were significantly lower in the model group than the control and Rg1 groups (P < 0.01, **Figure 4A-C**). The SOD, G6PDH, and CAT activities were significantly higher in the Rg1 group than the control group (P < 0.01, **Figure 4A-C**). The LPO levels were significantly higher in the model group than the control and Rg1 groups (P < 0.01, **Figure 4D**). However, the LPO was higher in the Rg1 group than the control group (P < 0.01, **Figure 4D**). The levels of Prdx1, SOD1, and SOD2 protein expression were significantly decreased in the model group in comparison to the Rg1 and control groups (P < 0.01, **Figure 4E**).

Rg1 promotes angiogenesis in steroid-induced ONFH rats

CD31 is one of the markers of endothelial cells, and it is often measured to determine angiogenesis. After immunostaining for CD31, MVD was calculated on a 200× field (**Figure 5D-F**). Endothelial cells that were clearly separated from the adjacent microvessels were counted as one microvessel. Only a few microvessels in

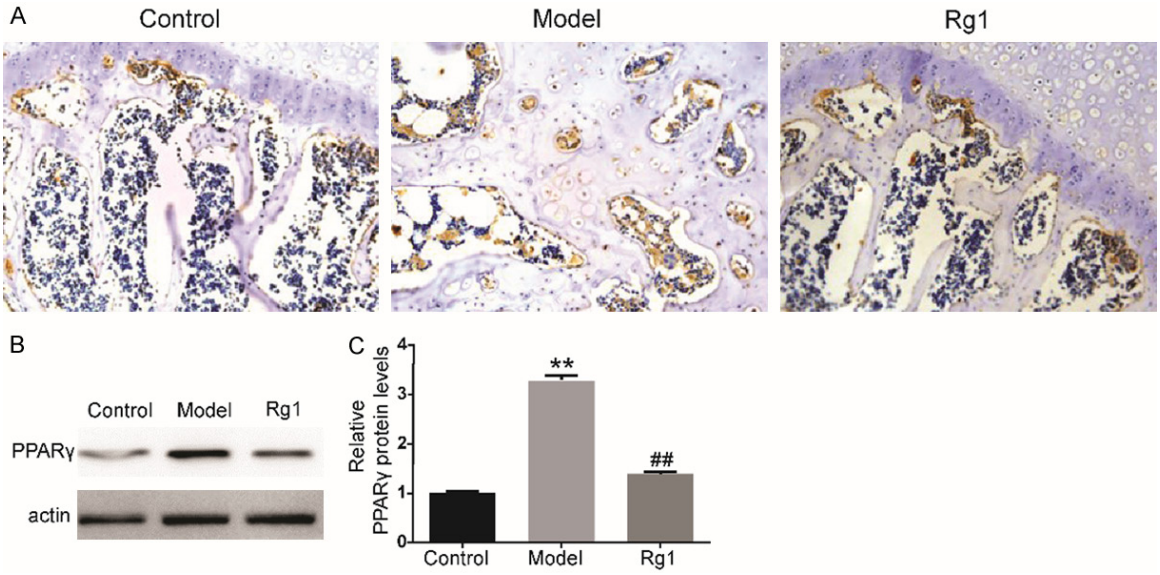

Figure 6. Rg1 reduces adipogenesis in steroid-induced ONFH rats. PPARγ immunoreactivity was significantly stronger in the steroid-induced ONFH group than the Rg1 and control groups (A). The PPARγ protein expression level was significantly higher in the model group than the Rg1 and control groups in Western blot analysis (B, C). The data are presented as the mean ± SD (n = 15 for the control, n = 15 for the model group, n = 15 for the Rg1 group). **: P < 0.01, in comparison to the control group. ##: P < 0.01, in comparison to the model group. Magnification: ×200 (A).

the subchondral bone of the necrotic femoral heads were observed in the model group (**Figure 5E**). In the Rg1 group, significantly more microvessels were present in the subchondral bone (**Figure 5F**). Significant statistical differences in MVD were found between the Rg1 group and the model group (P < 0.01, n = 15, **Figure 5G**). Furthermore, immunohistochemical staining for VEGF, which indicates potential angiogenic function (**Figure 5A-C**), was significantly lower in the model group than the control and Rg1 groups (P < 0.01, n = 15, **Figure 5H**).

Rg1 reduces adipogenesis in steroid-induced ONFH rats

We also performed immunohistochemical staining of PPARγ to evaluate adipogenesis in the femoral heads. As shown in **Figure 6A**, PPARγ was observed in the femoral heads of the rats in the model group, and the immunoreactivity was found to be more positive in that group than the control and Rg1 groups. As shown in **Figure 6B**, the level of PPARγ protein expression was significantly stronger in the model group than in the Rg1 and control groups. (P < 0.01, n = 15, **Figure 6C**).

Discussion

Glucocorticoid-induced osteonecrosis is a serious disease that can lead to the collapse of the femoral head, resulting in the need for total hip replacement [24]. Because the pathogenesis of steroid-induced ONFH is multifactorial, involving increased osteocyte apoptosis, skeletal angiogenesis, altered fat metabolism, fat embolism, and intravascular coagulation [25-27], none of the current treatment options have been proven to be the most effective. A large number of traditional Chinese herbal medicine have been used to treat bone diseases in recent years. Although Rg1 has been demonstrated to promote osteogenesis [11], its effect on steroid-induced ONFH remains unknown. The main findings of the present study were: (1) Rg1 protected steroid-induced ONFH by reducing osteonecrotic changes and inhibiting bone marrow adipogenesis; (2) Rg1 improved the microstructure of the trabecular bone and increased BMD in the femoral head of rats with steroid-induced ONFH; (3) Rg1 improved hyperlipidemia in steroid-induced ONFH rats; (4) Rg1 suppressed activated oxidative stress in steroid-induced ONFH in rats; (5) Rg1 enhanced femoral head neovascularization by preventing blood vessel loss in steroid-induced ONFH in rats; and (6) Rg1 suppressed the expression of PPARγ in the femoral heads of steroid-induced ONFH rats.

According to a previous study [5], high doses of glucocorticoids have been used to establish a

rat steroid-induced ONFH model. This model revealed crucial elements of clinical glucocorticoid-induced osteonecrosis, including the long-term complications of glucocorticoids and the importance of the dosing schedule. In the present study, during histopathological examination in the model group, we found that the empty lacunae ratio, which indicates pathogenesis in the early stage of ONFH, was significantly increased, and administration of Rg1 significantly decreased the adipose tissue area in the bone marrow and the empty lacunae ratio, implying improvement in fat metabolism due to Rg1. In this study, we first investigated the therapeutic effects of Rg1 on steroid-induced ONFH in rats.

Rg1 is an active ingredient extracted from a traditional Chinese herbal medicine, Panax ginseng. This herb has been found to attenuate fat accumulation, promote angiogenesis and suppress adipogenesis [28]. It is worth noting that a preclinical systematic review indicated that Rg1 is a promising neuroprotectant for Parkinson's Disease [29], suggesting its fundamental application value in the treatment of diseases. Glucocorticoid may decrease bone formation, induce hyperlipidemia, and increase adipogenesis in the bone marrow in the development of ONFH [30, 31].

In our study, the results of Micro-CT bone scanning showed that the BV/TV, Tb.Th, Tb.Pf, Tb.N, and BMD values were higher in the Rg1 treatment group than the model group. Thus, Rg1 may inhibit the loss of bone mass induced by administration of high-dose glucocorticoids. These results suggest that treatment with Rg1 promoted bone formation in the steroid-induced ONFH rats. Moreover, with the administration of Rg1, the TG, TC, LDL, ApoA1, and ApoB levels were significantly decreased and HDL was significantly increased in the Rg1 group in comparison to the model group. Our findings indicated that Rg1 could improve hyperlipidemia. In addition, we found that Rg1 significantly increased the levels of SOD, G6PDH, and CAT and decreased the LPO level in the Rg1 group in comparison to the model group. SOD, G6PDH, CAT, and LPO are important biomarkers against oxidative stress induced by glucocorticoid [32, 33]. The expression level of Prdx1, which is a member of the peroxiredoxin family that can encode antioxidant enzymes [34], was found to be significantly higher in the Rg1 group than the model group. This indicates that Rg1 might attenuate steroid-induced ONFH by reducing oxidative stress through Prdx1. Therefore, the results suggest that Rg1 could suppress steroid-induced oxidative stress during the development of osteonecrosis.

As previously reported, PPARγ is a nuclear receptor that can promote the differentiation of bone marrow stromal stem cells into adipocytes [35], limit oxidative stress [19], and inhibit osteoblastogenesis [36]; moreover, it might play a pivotal role in the pathogenesis of steroid-induced ONFH.

In the present study, PPARγ expression in the immunohistochemical staining and the protein levels in the model group were significantly increased, suggesting that steroid treatment may induce the adipogenic phenotype in steroid-induced ONFH rats. When Rg1 was administered, the expression of PPARγ was significantly decreased. We speculate that Rg1 might protect against steroid-induced ONFH by inhibiting adipogensis by suppressing the transactivation function of PPARγ. A previous study reported that PPARγ expression levels were decreased in oxidative stress-related diseases, such as diabetes [19], ischemic brain injury [20], and hypertension [37], and the activation of PPARγ could ameliorate oxidative stress and inflammation. In contrast, in our study, Rg1 suppressed oxidative stress and reduced the expression of PPARγ. The contradictory roles of PPARγ in oxidative stress in are not clearly understood; thus, further research is needed.

The inhibition of angiogenesis is one of the critical pathogenesis activities in steroid-induced ONFH. In the current study, we used MVD to measure the blood vessels in the femoral head. We identified a remarkable increase in MVD in the Rg1 group, suggesting the increase in vascularization of the femoral heads in rats treated with Rg1. CD31 and VEGF are biomarkers often used to determine angiogenesis [23, 38]. After immunohistochemical staining, CD31 and VEGF are significantly higher in the Rg1 group than the model group. These findings suggested that Rg1 might enhance angiogenesis of the femoral heads in steroid-induced ONFH rats. This is consistent with the results reported in

previous studies [39], which found that Rg1 can improve angiogenesis and promote vascular remodeling.

While the present study showed that the Rg1 could prevent steroid-induced osteonecrosis of the femoral head in rats, the exact mechanism still needs to be determined. The current study was only performed *in vivo*; it still needs to be determined whether Rg1 can affect vascular endothelial cells and mesenchymal stem cell differentiation *in vitro*.

In conclusion, our study indicated that Rg1 may enhance anti-oxidative stress and angiogenesis, inhibit adipogenesis and PPARγ expression in steroid-induced ONFH in rats. Our data suggest that treatment with Rg1 may be a potential therapeutic method for preventing steroid-induced ONFH.

Acknowledgements

This work was supported by the National Key Research and Development Program of China [2016YFC1304804] to XH. The authors gratefully acknowledge the generous support of the Collaborative Innovation Center for Cardiovascular Disease Translational Medicine of Jiangsu Province.

Disclosure of conflict of interest

None.

Address correspondence to: Xiao Han, Key Laboratory of Human Functional Genomics of Jiangsu Province, Nanjing Medical University, 101 Longmian Avenue, Jiangning District, Nanjing 211166, P. R. China. Tel: +86-25-8686-2898; Fax: +86-25-8686-2731; E-mail: hanxiao@njmu.edu.cn; Guoyong Yin, Department of Orthopedics, The First Affiliated Hospital of Nanjing Medical University, 300 Guangzhou Road, Nanjing 210029, P. R. China. E-mail: guoyong_yin@sina.com

References

[1] Ruiz-Arruza I, Barbosa C, Ugarte A and Ruiz-Irastorza G. Comparison of high versus low-medium prednisone doses for the treatment of systemic lupus erythematosus patients with high activity at diagnosis. Autoimmun Rev 2015; 14: 875-879.

[2] Bergmann TK, Barraclough KA, Lee KJ and Staatz CE. Clinical pharmacokinetics and pharmacodynamics of prednisolone and prednisone in solid organ transplantation. Clin Pharmacokinet 2012; 51: 711-741.

[3] Weinstein RS. Glucocorticoid-induced osteonecrosis. Endocrine 2012; 41: 183-190.

[4] Yang Z, Liu H, Li D, Xie X, Qin T, Ma J and Kang P. The efficacy of statins in preventing glucocorticoid-related osteonecrosis in animal models: a meta-analysis. Bone Joint Res 2016; 5: 393-402.

[5] Kuribayashi M, Fujioka M, Takahashi KA, Arai Y, Ishida M, Goto T and Kubo T. Vitamin E prevents steroid-induced osteonecrosis in rabbits. Acta Orthop 2010; 81: 154-160.

[6] Chen CF, Chiou WF and Zhang JT. Comparison of the pharmacological effects of panax ginseng and panax quinquefolium. Acta Pharmacol Sin 2008; 29: 1103-1108.

[7] Gao Y, Chu S, Shao Q, Zhang M, Xia C, Wang Y, Li Y, Lou Y, Huang H and Chen N. Antioxidant activities of ginsenoside Rg1 against cisplatin-induced hepatic injury through Nrf2 signaling pathway in mice. Free Radic Res 2017; 51: 1-13.

[8] Shin SS and Yoon M. Korean red ginseng (Panax ginseng) inhibits obesity and improves lipid metabolism in high fat diet-fed castrated mice. J Ethnopharmacol 2018; 210: 80-87.

[9] Gao Y, Chu S, Li J, Li J, Zhang Z, Xia C, Heng Y, Zhang M, Hu J, Wei G, Li Y and Chen N. Anti-inflammatory function of ginsenoside Rg1 on alcoholic hepatitis through glucocorticoid receptor related nuclear factor-kappa B pathway. J Ethnopharmacol 2015; 173: 231-240.

[10] Chen XC, Chen Y, Zhu YG, Fang F and Chen LM. Protective effect of ginsenoside Rg1 against MPTP-induced apoptosis in mouse substantia nigra neurons. Acta Pharmacol Sin 2002; 23: 829-834.

[11] Lu XZ, Wang JH, Wu X, Zhou L, Wang L, Zhang XW, Cao KJ and Huang J. Ginsenoside Rg1 promotes bone marrow stromal cells proliferation via the activation of the estrogen receptor-mediated signaling pathway. Acta Pharmacol Sin 2008; 29: 1209-1214.

[12] Gonzalez-Burgos E, Fernandez-Moriano C and Gomez-Serranillos MP. Potential neuroprotective activity of ginseng in Parkinson's disease: a review. J Neuroimmune Pharmacol 2015; 10: 14-29.

[13] Liu Y, Yi L, Wang L, Chen L, Chen X and Wang Y. Ginsenoside Rg1 protects human umbilical cord blood-derived stromal cells against tert-Butyl hydroperoxide-induced apoptosis through Akt-FoxO3a-Bim signaling pathway. Mol Cell Biochem 2016; 421: 75-87.

[14] Zhou T, Zu G, Zhang X, Wang X, Li S, Gong X, Liang Z and Zhao J. Neuroprotective effects of ginsenoside Rg1 through the Wnt/beta-ca-

tenin signaling pathway in both in vivo and in vitro models of Parkinson's disease. Neuropharmacology 2016; 101: 480-489.
[15] Yang Y, Li X, Zhang L, Liu L, Jing G and Cai H. Ginsenoside Rg1 suppressed inflammation and neuron apoptosis by activating PPAR-gamma/HO-1 in hippocampus in rat model of cerebral ischemia-reperfusion injury. Int J Clin Exp Pathol 2015; 8: 2484-2494.
[16] Leung KW, Ng HM, Tang MK, Wong CC, Wong RN and Wong AS. Ginsenoside-Rg1 mediates a hypoxia-independent upregulation of hypoxia-inducible factor-1alpha to promote angiogenesis. Angiogenesis 2011; 14: 515-522.
[17] Koh EJ, Kim KJ, Choi J, Jeon HJ, Seo MJ and Lee BY. Ginsenoside Rg1 suppresses early stage of adipocyte development via activation of C/EBP homologous protein-10 in 3T3-L1 and attenuates fat accumulation in high fat diet-induced obese zebrafish. J Ginseng Res 2017; 41: 23-30.
[18] Wang P, Wei X, Zhang F, Yang K, Qu C, Luo H and He L. Ginsenoside Rg1 of Panax ginseng stimulates the proliferation, odontogenic/osteogenic differentiation and gene expression profiles of human dental pulp stem cells. Phytomedicine 2014; 21: 177-183.
[19] Tol MJ, Ottenhoff R, van Eijk M, Zelcer N, Aten J, Houten SM, Geerts D, van Roomen C, Bierlaagh MC, Scheij S, Hoeksema MA, Aerts JM, Bogan JS, Dorn GW 2nd, Argmann CA and Verhoeven AJ. A PPARgamma-Bnip3 axis couples adipose mitochondrial fusion-fission balance to systemic insulin sensitivity. Diabetes 2016; 65: 2591-2605.
[20] Wu JS, Tsai HD, Cheung WM, Hsu CY and Lin TN. PPAR-gamma ameliorates neuronal apoptosis and ischemic brain injury via suppressing NF-kappaB-Driven p22phox transcription. Mol Neurobiol 2016; 53: 3626-3645.
[21] Ketsawatsomkron P and Sigmund CD. Molecular mechanisms regulating vascular tone by peroxisome proliferator activated receptor gamma. Curr Opin Nephrol Hypertens 2015; 24: 123-130.
[22] Kallai I, Mizrahi O, Tawackoli W, Gazit Z, Pelled G and Gazit D. Microcomputed tomography-based structural analysis of various bone tissue regeneration models. Nat Protoc 2011; 6: 105-110.
[23] Weidner N, Semple JP, Welch WR and Folkman J. Tumor angiogenesis and metastasis--correlation in invasive breast carcinoma. N Engl J Med 1991; 324: 1-8.
[24] Kamath AF, Sheth NP, Hosalkar HH, Babatunde OM, Lee GC and Nelson CL. Modern total hip arthroplasty in patients younger than 21 years. J Arthroplasty 2012; 27: 402-408.
[25] Jilka RL, Noble B and Weinstein RS. Osteocyte apoptosis. Bone 2013; 54: 264-271.
[26] Filipowska J, Tomaszewski KA, Niedzwiedzki L, Walocha JA and Niedzwiedzki T. The role of vasculature in bone development, regeneration and proper systemic functioning. Angiogenesis 2017; 20: 291-302.
[27] Zhang G, Qin L, Sheng H, Wang XL, Wang YX, Yeung DK, Griffith JF, Yao XS, Xie XH, Li ZR, Lee KM and Leung KS. A novel semisynthesized small molecule icaritin reduces incidence of steroid-associated osteonecrosis with inhibition of both thrombosis and lipid-deposition in a dose-dependent manner. Bone 2009; 44: 345-356.
[28] Heng Y, Zhang QS, Mu Z, Hu JF, Yuan YH and Chen NH. Ginsenoside Rg1 attenuates motor impairment and neuroinflammation in the MPTP-probenecid-induced parkinsonism mouse model by targeting alpha-synuclein abnormalities in the substantia nigra. Toxicol Lett 2016; 243: 7-21.
[29] Song L, Xu MB, Zhou XL, Zhang DP and Zhang SL. A preclinical systematic review of Ginsenoside-Rg1 in experimental Parkinson's disease. Oxid Med Cell Longev 2017; 2017: 2163053.
[30] Yu Z, Fan L, Li J, Ge Z, Dang X and Wang K. Lithium prevents rat steroid-related osteonecrosis of the femoral head by beta-catenin activation. Endocrine 2016; 52: 380-390.
[31] Hao C, Yang S, Xu W, Shen JK, Ye S, Liu X, Dong Z, Xiao B and Feng Y. MiR-708 promotes steroid-induced osteonecrosis of femoral head, suppresses osteogenic differentiation by targeting SMAD3. Sci Rep 2016; 6: 22599.
[32] Larocca M and Perna AM. Antioxidant and anti-inflammatory effects of cauliflower leaf powder-enriched diet against LPS induced toxicity in rabbits. Food Funct 2017; 8: 3288-3296.
[33] Inghilleri S, Morbini P, Oggionni T, Barni S and Fenoglio C. In situ assessment of oxidant and nitrogenic stress in bleomycin pulmonary fibrosis. Histochem Cell Biol 2006; 125: 661-669.
[34] Neumann CA, Krause DS, Carman CV, Das S, Dubey DP, Abraham JL, Bronson RT, Fujiwara Y, Orkin SH and Van Etten RA. Essential role for the peroxiredoxin Prdx1 in erythrocyte antioxidant defence and tumour suppression. Nature 2003; 424: 561-565.
[35] Cristancho AG and Lazar MA. Forming functional fat: a growing understanding of adipocyte differentiation. Nat Rev Mol Cell Biol 2011; 12: 722-734.
[36] Gu C, Xu Y, Zhang S, Guan H, Song S, Wang X, Wang Y, Li Y and Zhao G. miR-27a attenuates adipogenesis and promotes osteogenesis in steroid-induced rat BMSCs by targeting PPAR-gamma and GREM1. Sci Rep 2016; 6: 38491.

[37] Marchesi C, Rehman A, Rautureau Y, Kasal DA, Briet M, Leibowitz A, Simeone SM, Ebrahimian T, Neves MF, Offermanns S, Gonzalez FJ, Paradis P and Schiffrin EL. Protective role of vascular smooth muscle cell PPARgamma in angiotensin II-induced vascular disease. Cardiovasc Res 2013; 97: 562-570.

[38] Wang G, Zhang CQ, Sun Y, Feng Y, Chen SB, Cheng XG and Zeng BF. Changes in femoral head blood supply and vascular endothelial growth factor in rabbits with steroid-induced osteonecrosis. J Int Med Res 2010; 38: 1060-1069.

[39] Cheung LW, Leung KW, Wong CK, Wong RN and Wong AS. Ginsenoside-Rg1 induces angiogenesis via non-genomic crosstalk of glucocorticoid receptor and fibroblast growth factor receptor-1. Cardiovasc Res 2011; 89: 419-425.